An individual iron nanowire-filled carbon nanotube probed by micro-Hall magnetometry

K. Lipert,[1,2] S. Bahr,[1] F. Wolny,[1] P. Atkinson,[1] U. Weißker,[1] T. Mühl,[1] O. G. Schmidt,[1] B. Büchner,[1] and R. Klingeler[2,a)]
[1]*Leibniz Institute for Solid State and Materials Research IFW, 01069 Dresden, Germany*
[2]*Kirchhoff Institute for Physics, INF 227, D-69120 Heidelberg, Germany*

(Received 18 October 2010; accepted 4 November 2010; published online 22 November 2010)

We report on the magnetic properties of an individual, high-quality single-crystalline iron nanowire with diameter $d=26$ nm. The nanowire is embedded in a carbon nanotube which provides complete shielding against oxidation. Magnetization reversal is associated with domain wall formation where domain nucleation is initiated by curling. The observed nucleation fields of up to 900 mT are much higher than reported previously and nearly reach the shape anisotropy field of iron nanowires. © *2010 American Institute of Physics*. [doi:10.1063/1.3520146]

The properties of individual nanoscale magnets have attracted much attention over the past two decades, in part motivated by potential applications such as spintronic nanodevices, high density magnetic data storage, and biomedical applications.[1–9] Iron nanostructures form an ideal test system to study the effect of size reduction on magnetic properties. In addition, iron nanowires exhibit stable magnetization vectors and well separated magnetic poles which renders them attractive for various applications, e.g., in magnetic force microscopy (MFM) or cell manipulation.[10–12] However, iron's strong tendency to oxidize is a serious drawback, both for fundamental investigations and application of iron based nanomagnets. The solution is to use iron nanowires encapsulated in diamagnetic carbon nanotubes (CNT) which shield the enclosed material but do not affect its ferromagnetic properties.

We investigate here the magnetic properties of a high-quality 26 nm diameter Fe nanowire encapsulated inside a multiwalled CNT. Due to the large aspect ratio, the shape anisotropy $(\mu_0 M_s^2/4 \approx 0.96\ \mathrm{MJ/m^3})$ clearly exceeds the magnetocrystalline anisotropy $(\approx 0.048\ \mathrm{MJ/m^3})$ so that the easy magnetic axis is oriented along the wire. This has been confirmed by MFM studies for the wires studied here.[13] The magnetic properties were investigated by micro-Hall magnetometry which has a potential sensitivity of up to $10^4\ \mu_B$.[14,15] We used a two-dimensional electron gas confined in an n-type GaAs/AlGaAs modulation doped heterostructure 90 nm below the surface to measure the magnetic stray fields of an individual nanowire. The carrier concentration and mobility were $n=1.7\times 10^{11}\ \mathrm{cm^{-2}}$ and $\mu=7\times 10^5\ \mathrm{cm^2/V\ s}$, respectively, at $T=1.5$ K. The device was patterned by electron beam lithography and wet chemical etching to achieve an active area of $\approx 0.8\times 0.8\ \mu\mathrm{m}^2$ on the sensor surface. The Hall coefficient $R_H=4.8\ \mathrm{k\Omega/T}$ only very weakly changed in the temperature range 6 K$\leq T \leq$60 K and magnetic field range $B\leq 1$ T under study.

Fe-CNTs were grown on a Si substrate by thermal chemical vapor deposition as reported previously.[16] X-ray diffractometry and transmission electron microscopy confirm that the Fe-CNTs mainly contain single crystalline (ferromagnetic) α-Fe. A Kleindieck three-axis micromanipulation system inside a scanning electron microscope (SEM) was utilized to select a single high-purity, catalyst-free, and homogeneously filled Fe-CNT. It was placed with a precision of a few tens of nanometers on the active area of the magnetometer forming an angle of $\approx 12°$ with respect to the surface (Fig. 1). Magnetic fields were applied in the sensor-plane and the angle Θ between nanotube and magnetic field was varied by rotation of the device.

Our experimental setup probes the Hall voltage generated by the Fe-CNT's magnetic stray field z-component B_Z (perpendicular to the sensor surface) penetrating the active area of the sensor as a function of an external magnetic field. Our local measurement technique is mainly sensitive to the stray field at one end of the magnetic wire. Since MFM studies under applied magnetic fields on our nanowires (see, e.g., Ref. 13) have clearly confirmed that the remanent magnetization state is always a single domain state the data can be straightforwardly attributed to the magnetic properties of the entire wire. Data are obtained at field sweeping rates $\nu=0.1-0.4$ T/min at various temperatures T and angles Θ of the external magnetic field $\mu_0 H$ direction with respect to the Fe-CNT long axis. Typical results of magnetization loops are shown in Fig. 2. At large angles [Fig. 2(a)], the curves are rectangular and the main features are sharp jumps of $\langle B_Z \rangle$

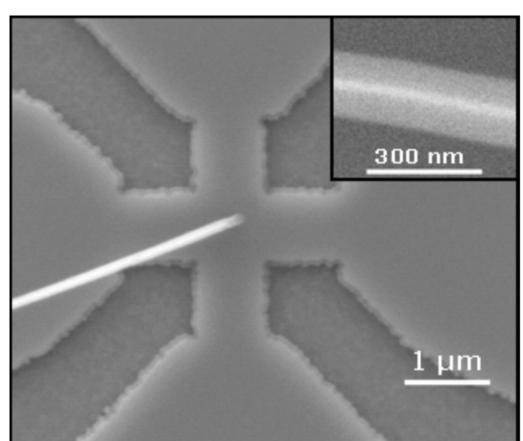

FIG. 1. SEM image of the 26 nm in diameter iron nanowire inside the CNT placed at the center of the $0.8\times 0.8\ \mu\mathrm{m}^2$ Hall device. Inset: SEM back scattered image of the Fe-CNT.

[a)]Electronic mail: klingeler@kip.uni-heidelberg.de.

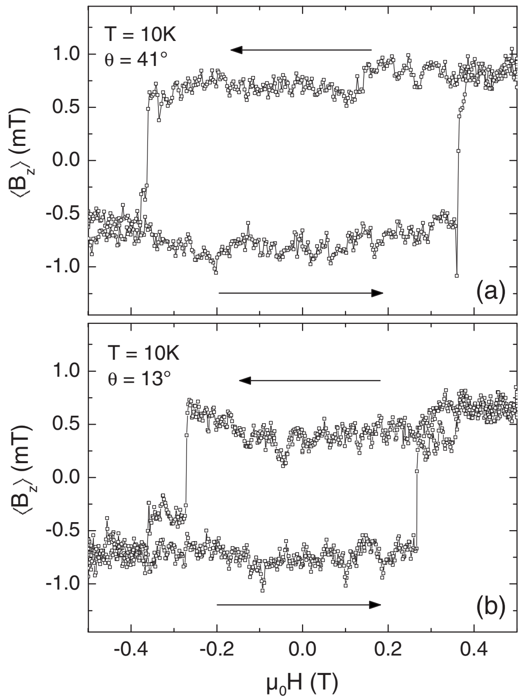

FIG. 2. Average magnetic stray field $\langle B_Z \rangle$ as detected by the μ-Hall magnetometer vs external magnetic field H, at $T=10$ K. (a) Square shaped hysteresis loop with singular jumps, measured at $\Theta=41°$. (b) Hysteresis loop at $\Theta=13°$ with two steps.

which are symmetric with respect to $H=0$. These jumps at fields H_n are associated with magnetization reversal of the encapsulated nanowire. We note that this behavior resembles single domain particle magnetization reversal. At small angles $|\Theta| \leq 37°$, however, the magnetization loops reproducibly exhibit additional small jumps which will be discussed below in terms of nucleation of a domain with reversed magnetization at H_n followed by domain wall depinning at slightly higher fields [Fig. 2(b)].

Upon changing the angle Θ of the applied magnetic field we observe a strong change of $\langle H_n \rangle$ as summarized in Fig. 3. At small angles, magnetization reversal only moderately depends on Θ and we find $\mu_0 \langle H_n \rangle \approx 265$ mT. For $\Theta > 45°$, however, there is a strong increase of $\langle H_n \rangle$ and very high nucleation fields are observed when $\Theta \to 90°$. In nearly perpendicular configuration a maximum $\mu_0 \langle H_n \rangle$ of 891 mT is

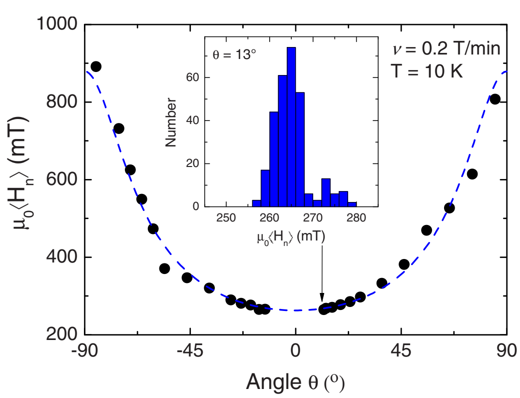

FIG. 3. (Color online) Angular variation of the mean nucleation field $\langle H_n \rangle$. Each point is the average of ≥ 10 sweeps. The line corresponds to $\langle H_n \rangle$ as predicted in the curling model by Eq. (1). Inset: Histogram of nucleation fields for 280 switching events taken at $\Theta=13°$ and $T=10$ K.

found which is close to the theoretically predicted shape anisotropy field ($\mu_0 H_A = 2K_1/M_s$) of about 1.1 T for an infinitely long iron cylinder.[17] Recalling that, e.g., imperfections reduce the experimentally observed nucleation fields in any real material, this finding confirms the extraordinary high quality of the iron nanowire inside the CNT.

The angular variation of $\langle H_n \rangle$ (Fig. 3) is typical for switching via the curling mode in ferromagnetic nanowires. In this model, $\langle H_n \rangle(\Theta)$ for infinitely long ferromagnetic cylinders is described by[18]

$$H_n = \frac{M_s}{2} \frac{a(1+a)}{\sqrt{a^2 + (1+2a)\cos^2(\Theta)}}. \tag{1}$$

Here, M_s is the saturation magnetization of iron and $a=-1.08(d_0/d)^2$, where d denotes the nanowire's diameter and $d_0 = 2\sqrt{A/(\mu_0 M_s^2)}$ is the so-called exchange length depending on the exchange constant A. Describing the data in terms of Eq. (1) reveals a good agreement with the experimentally observed angular dependence of $\langle H_n \rangle$ (cf. line in Fig. 3). Quantitatively, fitting yields $d_0 = 12$ nm and $\mu_0 M_s = 2.2$ T which agrees well with literature data.[19]

While the experimental data $\langle H_n \rangle(\Theta)$ nicely agree to the curling model for an infinitely long nanowire, the observation of a second step in $M(H)$ at small angles [Fig. 2(b)] implies a more complex scenario. We recall that in real systems even for high-quality nanowires the localized magnetization reversal mechanism is often favored.[20,21] Here, nucleation of a magnetic domain with reversed magnetization and a corresponding domain wall appears at the end of the nanowire. Accordingly, complete magnetic switching is associated with rapid domain wall motion through the nanowire. This scenario is supported by the observed additional magnetization steps at small angles [Fig. 2(b)]. The data imply a two-step process starting with domain nucleation at $\langle H_n \rangle$ while the additional step is probably associated with the depinning of a domain wall. For the Fe-CNT at hand, tiny diameter fluctuations, structural defects, impurities, and effects of the wire ends might cause such pinning. Depinning is associated with a well defined energy and a higher magnetic field has to be applied to overcome the pinning and to complete the switching process. At large angles where H_n is higher than the depinning field the second step is not observed.

A detailed study of the distribution of nucleation fields (inset of Fig. 3) provides further evidence for this scenario. At low temperatures the distribution of nucleation fields splits into two well separated parts while no splitting occurs at higher temperatures $T \geq 20$ K. This splitting implies at least two reversed domain nucleation sites characterized by different energy barriers which become distinct at low temperatures.

Finally, we discuss the temperature dependence of $\langle H_n \rangle$ as displayed in Fig. 4 for a fixed angle $\Theta=13°$, i.e., in the two-step regime of $M(H)$. As expected for a thermally activated process, the nucleation field decreases upon heating. Quantitatively, in the thermal activation regime the mean nucleation field is described by[22]

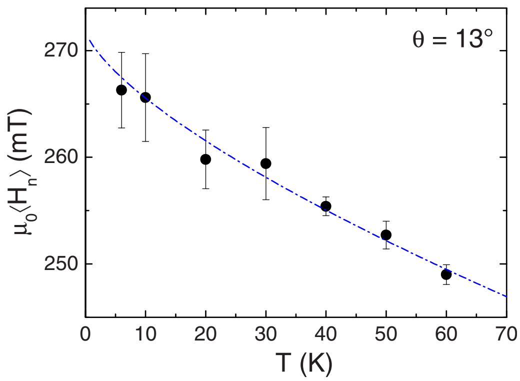

FIG. 4. (Color online) Temperature dependence of the mean nucleation field $\langle H_n\rangle$ with error bars corresponding to the standard deviation. The dotted line is a fit according to Eq. (2).

$$\langle H_n\rangle = H_0\left\{1-\left[\frac{k_B T}{E_0}\ln(cT/\nu)\right]^{2/3}\right\}, \tag{2}$$

where H_0 is the nucleation field at $T=0$, k_B the Boltzmann constant, E_0 the mean energy barrier at $H=0$, $\nu=3.3$ mT/s the sweeping rate of the magnetic field and $c=k_B H_0/(E_0\tau_0)$, with τ_0 the prefactor of the thermal activation rate. We use $\tau_0=1.2\times10^{-10}$ s.[23] Fitting the experimental data by means of Eq. (2) yields $E_0/k_B=5.18\times10^4$ K and $\mu_0 H_0=272$ mT. The activation volume $V=E_0/(\mu_0 M_s H_0)$ derived from E_0 only amounts to $V=1.5\times10^3$ nm^3. This volume is much smaller than the one of the nanowire ($\approx 8\times10^6$ nm^3) which again implies that the reversal starts in a small region of the wire, consistent with domain nucleation.

Although the angular dependence of $\langle H_n\rangle$ indicates the evolution of curling modes, there is compelling evidence of localized magnetization reversal via domain wall formation and propagation. The latter observation is consistent with the conjecture that any arbitrarily weak inhomogeneity can lead to a localization of the nucleation mode and shows that the actual degree of localization strongly depends on the nanowire's structure.[20] In contrast to other experimental work[24,25] where magnetization data deduced from magnetoresistance measurements of Ni and Co nanowires only reproduce the curling model for angles <50°, our data agree with the curling model for large angles, too. This is somewhat surprising, as theoretical calculations[18,26] suggest a transition from curling to coherent rotation at a certain angle Θ which we do not observe in our studies. Our data hence suggest a scenario in which switching starts by the nucleation of a small domain with reversed magnetization according to the curling model where inhomogeneities may lead to domain wall pinning followed by a domain wall propagation. Depending on Θ, the depinning field may be higher than the curling instability.

In conclusion, we have investigated the magnetic properties (temperature and angular dependence of the nucleation fields) of a long CNT-coated single crystalline Fe nanowire with diameter $d=26$ nm by means of micro-Hall magnetometry. The angular dependence of the nucleation field is in good agreement with the curling model for infinitely long ferromagnetic nanowires. However, the observation of additional magnetization steps at small angles, the distribution of the nucleation fields, and our analysis of the temperature dependence provide good experimental evidence that magnetization reversal is associated with reversed domain nucleation, supporting a scenario where domain formation is initiated by curling. At angles Θ close to 90° we detect extraordinary high nucleation fields (up to 900 mT) near the theoretical limit, implying that Fe-CNT is a very promising nanomaterial for applications where environmentally protected nanomagnets with extreme anisotropy are demanded.

Work was supported by the EC (CARBIO: MRTN-CT-2006-035616) and the DFG (Grant No. KA1694/5). We thank Nanonic GmbH Co. and J. Biberger for technical support and C. Linz for contacting the two-dimensional electron gas. Valuable discussions with P. Das and J. Müller are gratefully acknowledged.

[1] Y. Song, A. L. Schmitt, and S. Jin, Nano Lett. **8**, 2356 (2008).
[2] G. S. D. Beach, C. Nistor, C. Knutson, M. Tsoi, and J. L. Erskine, Nature Mater. **4**, 741 (2005).
[3] R. J. Mannix, S. Kumar, F. Cassiola, M. Montoya-Zavala, E. Feinstein, M. Prentiss, and D. E. Ingber, Nat. Nanotechnol. **3**, 36 (2008).
[4] V. K. Varadan, L. Chen, and J. Xie, *Nanomedicine* (Wiley, Chichester, 2008).
[5] R. Klingeler, S. Hampel, and B. Büchner, Int. J. Hyperthermia **24**, 496 (2008).
[6] A. Taylor, Y. Krupskaya, K. Kramer, S. Fussel, R. Klingeler, B. Büchner, and M. P. Wirth, Carbon **48**, 2327 (2010).
[7] J. H. Lee, Y. M. Hun, Y. W. Jun, J. W. Seo, J. T. Jang, H. T. Song, S. Kim, E. J. Cho, H. G. Yoon, J. S. Suh, and J. Cheon, Nat. Med. **13**, 95 (2007).
[8] C. G. Hadjipanayis, M. J. Bonder, S. Balakrishnan, X. Wang, H. Mao, and G. C. Hadjipanayis, Small **4**, 1925 (2008).
[9] L. Mohaddes-Ardabili, H. Zheng, S. B. Ogale, B. Hannoyer, W. Tian, J. Wang, S. E. Lofland, S. R. Shinde, T. Zhao, Y. Jia, L. Salamanca-Riba, D. G. Schlom, M. Wuttig, and R. Ramesh, Nature Mater. **3**, 533 (2004).
[10] A. Hultgren, M. Tanase, C. S. Chen, G. J. Meyer, and D. H. Reich, J. Appl. Phys. **93**, 7554 (2003).
[11] F. Wolny, U. Weissker, T. Mühl, A. Leonhardt, S. Menzel, A. Winkler, and B. Büchner, J. Appl. Phys. **104**, 064908 (2008).
[12] F. Wolny, T. Mühl, U. Weissker, A. Leonhardt, U. Wolff, D. Givord, and B. Büchner, J. Appl. Phys. **108**, 013908 (2010).
[13] M. U. Lutz, U. Weissker, F. Wolny, C. Müller, M. Löffler, T. Mühl, A. Leonhardt, B. Büchner, and R. Klingeler, J. Phys.: Conf. Ser. **200**, 072062 (2010).
[14] Y. Li, C. Ren, P. Xiong, S. von Molnár, Y. Ohno, and H. Ohno, Phys. Rev. Lett. **93**, 246602 (2004).
[15] S. Bahr, K. Petukhov, V. Mosser, and W. Wernsdorfer, Phys. Rev. Lett. **99**, 147205 (2007).
[16] A. Leonhardt, S. Hampel, C. Müller, I. Mönch, R. Koseva, M. Ritschel, K. Biedermann, and B. Büchner, Chem. Vap. Deposition **12**, 380 (2006).
[17] R. Skomski, *Simple Models of Magnetism* (Oxford University Press, New York, 2008).
[18] A. Aharoni, J. Appl. Phys. **82**, 1281 (1997).
[19] M. E. Schabes, J. Magn. Magn. Mater. **95**, 249 (1991).
[20] R. Skomski, Phys. Rev. B **62**, 3900 (2000).
[21] W. Wernsdorfer, B. Doudin, D. Mailly, K. Hasselbach, A. Benoit, J. Meier, J.-Ph. Ansermet, and B. Barbara, Phys. Rev. Lett. **77**, 1873 (1996).
[22] L. Gunther and B. Barbara, Phys. Rev. B **49**, 3926 (1994).
[23] P. Banerjee, F. Wolny, D. V. Pelekhov, M. R. Herman, K. C. Fong, U. Weissker, T. Mühl, Yu. Obukhov, A. Leonhardt, B. Büchner, and P. C. Hammel, Appl. Phys. Lett. **96**, 252505 (2010).
[24] J.-E. Wegrowe, D. Kelly, A. Franck, S. E. Gilbert, and J.-Ph. Ansermet, Phys. Rev. Lett. **82**, 3681 (1999).
[25] R. A. Silva, T. S. Machado, G. Cernicchiaro, A. P. Guimarães, and L. C. Sampaio, Phys. Rev. B **79**, 134434 (2009).
[26] J. Escrig, M. Daub, P. Landeros, K. Nielsch, and D. Altbir, Nanotechnology **18**, 445706 (2007).